Received: 24 February 2019 | Revised: 6 October 2019 | Accepted: 4 November 2019

DOI: 10.1002/psc.3234

RESEARCH ARTICLE

WILEY Journal of PeptideScience

Effect of oligoarginine conjugation on the antiwrinkle activity and transdermal delivery of GHK peptide

Ga-Hee Hur[1] | Sang-Cheol Han[2] | A-Reum Ryu[1] | Youngsic Eom[1] | Jhin-Wook Kim[2] | Mi-Young Lee[1,3]

[1] Department of Medical Sciences, Soonchunhyang University, Asan, Republic of Korea

[2] Department of Material Laboratory, Dermafirm Co., Ltd., Wonju, Republic of Korea

[3] Department of Medical Biotechnology, Soonchunhyang University, Asan, Republic of Korea

Correspondence
Mi-Young Lee, Department of Medical Biotechnology, Soonchunhyang University, Asan, Chungnam 31538, Republic of Korea.
Email: miyoung@sch.ac.kr

Funding information
Soonchunhyang University; National Research Foundation of Korea, Grant/Award Number: 2018H1D2A2010318

GHK (Gly-His-Lys), a natural peptide found in human skin and plasma, has been widely used in the cosmeceutical and pharmaceutical fields. The hydrophilic GHK and GHK-Cu are limited in their abilities to penetrate deeply into skin; because of this, various strategies for their skin delivery have been developed. In this investigation, Arg_4 was conjugated with GHK to get heptapeptide, GHK-R4, and then in vitro antiwrinkle activity and transdermal delivery were compared between GHK and GHK-R4. Notably, Arg_4 conjugation accelerated the cellular penetration of GHK both in vitro and in vivo. Furthermore, higher in vitro antiwrinkle activity and collagen biosynthesis was obtained with GHK-R4 at much lower doses than with control R4-free GHK. The enhanced activity and delivery of GHK-R4 might be due to the cell penetrating ability and matrix metalloproteinase (MMP) inhibitory activity of R4 itself.

1 | INTRODUCTION

GHK (Gly-His-Lys), a naturally occurring peptide motif in human skin, plasma, and urine, has been used for wound healing and skin care.[1] The GHK sequence is not only present in the alpha 2 (I) chain of type I collagen but also released from damaged proteins by proteolysis during wound healing.[2] GHK has a strong affinity for copper, forming GHK-Cu, improving its bioavailability. Copper plays a prime role in the stimulation of several enzymes associated with tissue repair and collagen biosynthesis.[3,4] The biological activities of GHK and copper-bound GHK (GHK-Cu) include skin regeneration, wound healing, antioxidant, anti-inflammation, antilung injury, DNA/protein repair, and anticancer.[1,5]

A wide variety of data show that GHK is able to bind not only with copper but also with heparin and heparin sulfate, facilitating its involvement in cell adhesion, extracellular matrix structure, the stimulation of cell migration, and differentiation.[6] GHK (with or without copper) is functional starting from picomolar concentrations; however, much higher levels of GHK have been required clinically because of its low delivery through skin.[2] As a general rule, only lipophilic molecules with a molecular weight below 500 Da are able to passively permeate through the skin.[2] Thus, hydrophilic GHK and GHK-Cu have difficulty in penetrating into skin,[7] although they can pass through the lipid barrier of the stratum corneum and reach epidermal cells.[8]

In both cosmetic and drug delivery, extensive work has been done to overcome the barrier for dermal or transdermal delivery, facilitating more efficient penetration into the deeper layers of the skin, sufficient to reach the systemic circulation.[9-11] While there are many reports on GHK-Cu to date, fewer data on GHK without copper are available. However, all the available evidence is consistent with GHK exerting its biological effects as GHK-Cu.[2]

Currently, incidences of contact dermatitis by copper exposure have been reported, although GHK-Cu has a low potential for skin irritation.[12] Considering the diverse cosmeceutical potential of GHK, it is important to provide safest and most efficient alternative with enhanced skin absorption and biological activity. Therefore, we investigated whether Arg_4 conjugation might accelerate the skin penetration of GHK in vitro and in vivo. Furthermore, the enhancement of antiwrinkle activity and collagen biosynthesis of GHK via Arg_4 conjugation in UVB-induced fibroblasts were also investigated.

2 | MATERIALS AND METHODS

2.1 | Peptide synthesis

All peptides were synthesized using standard Fmoc solid-phase peptide synthesis with 2-chlorotrityl (CTL) resin. The procedure includes three steps: synthesis of H-Arg (Pbf)Arg (Pbf)Arg (Pbf)Arg (Pbf)-CTL-resin **1**, synthesis of H-ArgArgArgArg-OH **2**, and synthesis of H-GlyHisLys-ArgArgArgArg-OH **3**. To synthesize H-Arg (Pbf)Arg (Pbf)Arg (Pbf)Arg (Pbf)-CTL-resin **1**, 7 g (10 mmoles) CTL resin (BeadTech, Korea, 1% DVB cross-linked, 100-200 mesh, 1.41 mmol/g) was added to the reactor and then swelled using methylene chloride (MC) and dimethylformamide (DMF) sequentially. After reaction with Fmoc-Arg (Pbf)-OH, 6.4 g (10 mmol, 1 eq) and *N,N′*-diisopropyl ethylamine (DIPEA) 5.3 mL (3 eq) in DMF 40 mL. After the capping reaction in MC: MeOH: DIPEA (17:2:1), deblocking was performed in 20% piperidine in DMF. The elongation of Arg (Pbf) was performed using HBTU (3-[bis (dimethylamino)methyliumyl]-3*H*-benzotriazol-1-oxide hexafluorophosphate) and HOBt (*N*-hydroxybenzotriazole). To synthesize H-ArgArgArgArg-OH (R4) **2**, cleavage and deprotection of **1** was performed in a solution of 95% trifluoroacetic acid (TFA), 2.5% MC, and 2.5% water for 3 hours. After the resin was filtered and washed with a small volume of MC to collect the cleaved peptide in filtrate, the combined filtrate was then evaporated under reduced pressure, and the resulting residue was precipitated in 100 mL of cold ether. After filtering, the crude peptide was dissolved in 40 mL distilled water and purified by Prep-LC (column ID 5 cm) and then freeze dried to yield **2** (1.7 g, yield 26.6%, purity 99.1% by high-performance liquid chromatography [HPLC]) as a white powder. The molecular weight of the final product was measured as 643.0 (M+1, calculated MW: 642.4) by liquid chromatography–mass spectrometry (LC-MS). To synthesize H-GlyHisLys-ArgArgArgArg-OH **3**, the peptide on resin **1** was elongated further with protected amino acids (Fmoc-Lys (Boc)-OH, Fmoc-His (Trt)-OH, and Boc-Gly-OH in that order. Resin **3** was cleaved and deprotected in cleavage cocktail solution for 3 hours; the crude peptide was purified with Prep-LC (column ID 5 cm) and then freeze dried to yield **4** (3.6 g, yield 37.3%, purity 99.2% by HPLC) as white powder. The molecular weight of the final product was measured as 965.60 (M +1, calculated MW: 964.59) by LC-MS. The synthesized peptides were acetate form of GHK (GHK-acetate), GHK-R4, and R4.

2.2 | Cell culture, viability, and proliferation

Hs68 human dermal fibroblasts were purchased from the American Type Culture Collection (Manassase, Virginia) and cultured in monolayers at 37°C in 5% CO_2 in Dulbecco's modified Eagle's medium (DMEM) containing 10% fetal bovine serum (FBS). Hs68 cells (1×10^5 cells/well) were seeded in a 6-well plate (Falcon, Corning, New York) for 24 hours and then UVB irradiated (200 mJ/cm^2, 312 nm) (VL.215-LM, Vilber Lourmat, Eberhardzell, Germany). After UVB irradiation, the cells were treated with various concentrations of peptides in medium containing 1% serum for 48 hours. After GHK and GHK-R4 treatment for 24 hours, Hs68 cells were treated with MTT [3-(4,5-dimethylthiazol-2-yl)-2,5-diphenyl tetrazolium bromide] to determine viability. After formazan formation by MTT, 50 μL DMSO was added and the absorbance was measured at 570 nm. The proliferative effects of the peptide on Hs68 cells were determined by WST assay. Briefly, cells were cultured for 24 hours, and then cells in DMEM containing 1% FBS were treated with various concentrations of peptides for 48 or 72 hours. WST-1 solution diluted in phosphate-buffered saline (PBS) at a ratio of 1:10 was then reacted with the cells in the dark for 3 hours. The absorbance was measured at 450 nm.

2.3 | Fluorescent labeling of peptide with FAM

FAM (6-carboxyfluorescein) in DMSO was slowly added dropwise into the peptide solution in 0.1 M bicarbonate buffer pH 9.0. The molar ratio of FAM to peptide was 1:5. The reaction mixture was incubated at room temperature (RT) for 2 hours in the dark and then dialyzed and concentrated.

2.4 | In vitro penetration of GHK and GHK-R4

The cellular uptake of GHK and GHK-R4 in Hs68 fibroblast was compared upon conjugating with FAM. Hs68 cells were treated with 50 μM fluorescent GHK and GHK-R4 for 1 or 3 hours. The cells were washed twice with PBS and then filled with DMEM until observed.[13] The prepared cells were then observed by confocal microscope (Olympus, Tokyo, Japan), and the images were recorded.

2.5 | In vivo penetration of GHK and GHK-R4

The protocol was approved by the Animal Research Ethics Committee at Soonchunhyang University, approval number: SCH18-0062. SKH-1 hairless mice (male, 6 weeks old) were obtained from Orient Bio (Seongnam, Korea). On the day of the experiment, GHK and GHK-R4 in DMEM were applied to approximately 2 cm^2 of the skin on the back of each mouse. At 1, 2, 4, and 6 hours postapplication, the mice were euthanized and the area of application was dissected. The sample was placed in 10% formalin for 24 hours, then embedded in Tissue-Tek OCT compound (Sakura Finetek, Torrance, California), and sectioned using a cryostat microtome (Leica, Wetzlar, Germany). The skin sections (14 μm) were mounted on glass slides. The slides were visualized without any additional staining or treatment with a 10× objective using a confocal microscope (Olympus, Tokyo, Japan) equipped with a filter for Alexa Fluor488 and FV10-ASW software.

2.6 | Sircol collagen assay

Total soluble collagen in Hs68 cell culture supernatant was quantified using the Sircol collagen assay (Biocolor, Belfast, UK). UVB-irradiated Hs68 cells were incubated for 48 hours with GHK or GHK-R4. One milliliter of Sirius red dye, an anionic dye that reacts specifically with the basic side chain groups of collagens under assay conditions, was

added to 400 μL of cell culture medium supernatant and incubated with gentle rotation for 30 minutes at RT. After centrifugation, the pellet was washed with ice-cold acid-salt wash reagent, released in alkali reagent, and the absorbance at 570 nm was measured by ELISA (Sunrise, Tecan, Männedorf, Switzerland). The amount of collagen was calculated on the basis of the standard curve obtained with bovine type I collagen supplied with the kit.

2.7 | Elastase inhibition assay

Elastase inhibition was measured using porcine pancreatic elastase (Sigma, St. Louis, Missouri) and *N*-succinyl-Ala-Ala-Ala-*p*-nitroanilide as a substrate. The reaction mixture contained 200 mM Tris-HCl buffer (pH 8.0), 0.1 U/mL elastase, and 3.2 mM *N*-succinyl-Ala-Ala-Ala-*p*-nitroanilide. The mixture was incubated for 10 minutes at 37°

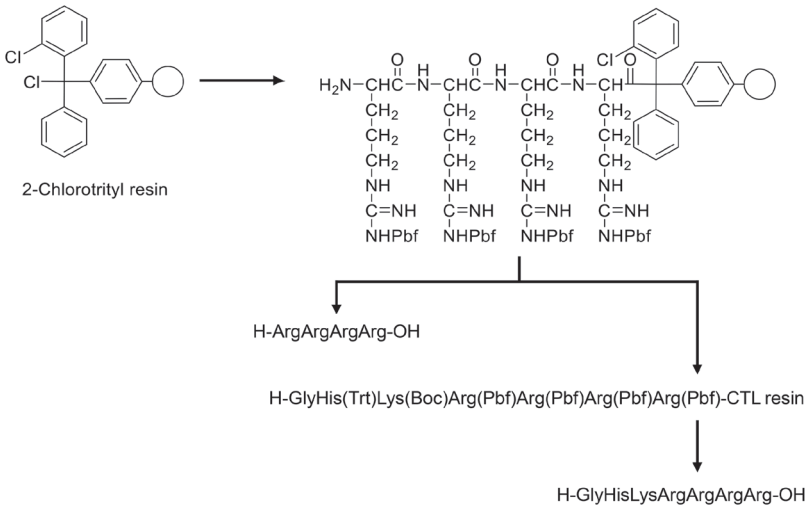

FIGURE 1 The scheme for the synthesis of GHK (GHK-acetate form) and GHK-R4 by using standard Fmoc chemistry-based solid peptide synthesis with 2-chlorotrityl resin

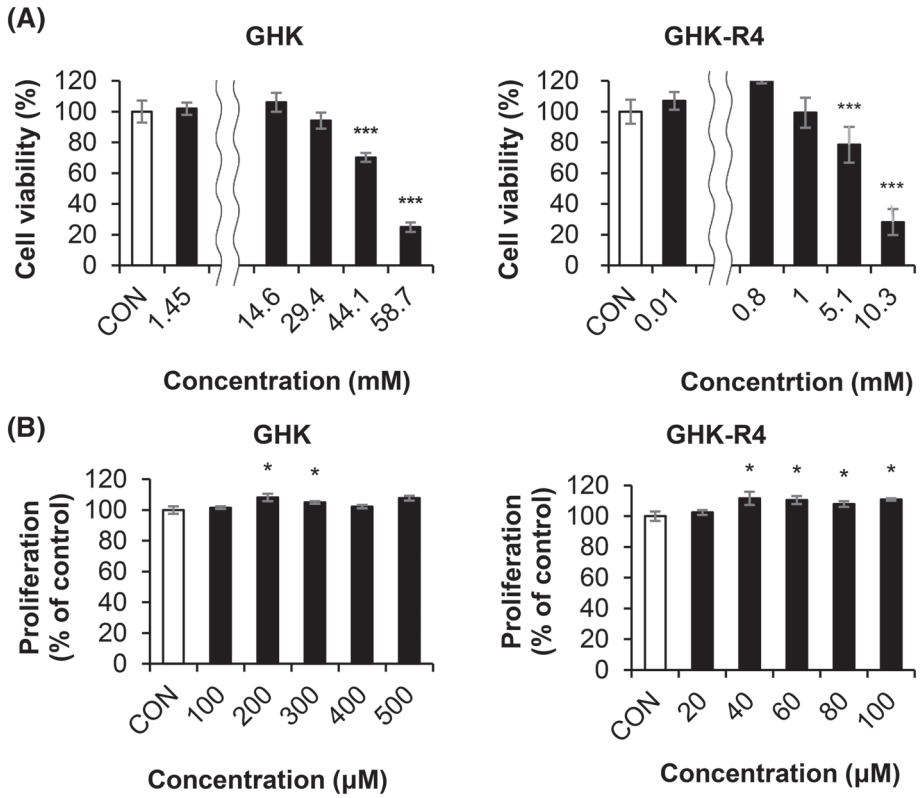

FIGURE 2 (A) Effect of cell viability of GHK and GHK-R4 on Hs68 fibroblast cells. Cell viability was determined by MTT assay. $^{***}P < .05$ compared with control. (B) Proliferative activity of GHK and GHK-R4 on the proliferation of fibroblasts, measured by the WST-1 assay. $^{*}P < .05$ compared with control

C after adding the peptide. The release of *p*-nitroaniline was measured at 410 nm using a 96-well plate reader.

2.8 | Gelatin zymography

MMP-2 secreted into the culture medium was measured by gelatin zymography. Hs68 fibroblast cell medium was collected after GHK, GHK-R4, and R4 treatment. The supernatant samples were mixed with standard SDS-PAGE gel loading buffer without β-mercaptoethanol and loaded on the gel without heat denaturation. Samples were separated by SDS-PAGE through 8% gel containing 0.1% gelatin at 90 V for 2 hours. After electrophoresis, the gel was washed twice with 2.5% Triton X-100 on a shaker for 1 hour at RT to remove the SDS. The gel was then incubated in 50 mL reaction buffer (50 mM Tris-HCl, pH 7.5, containing 10 mM $CaCl_2$ and 0.15 M NaCl) at 37°C overnight, stained with brilliant blue R-250, and destained with methanol-acetic acid in distilled water.

2.9 | Western blot analysis

Whole-cell lysates were prepared, and samples containing 25 μg of total protein were separated on 8% to 10% SDS-PAGE gels and then transferred onto polyvinylidene difluoride (PVDF) membranes for 1 hour at 400 mA. After transfer, the membranes were blocked for 2

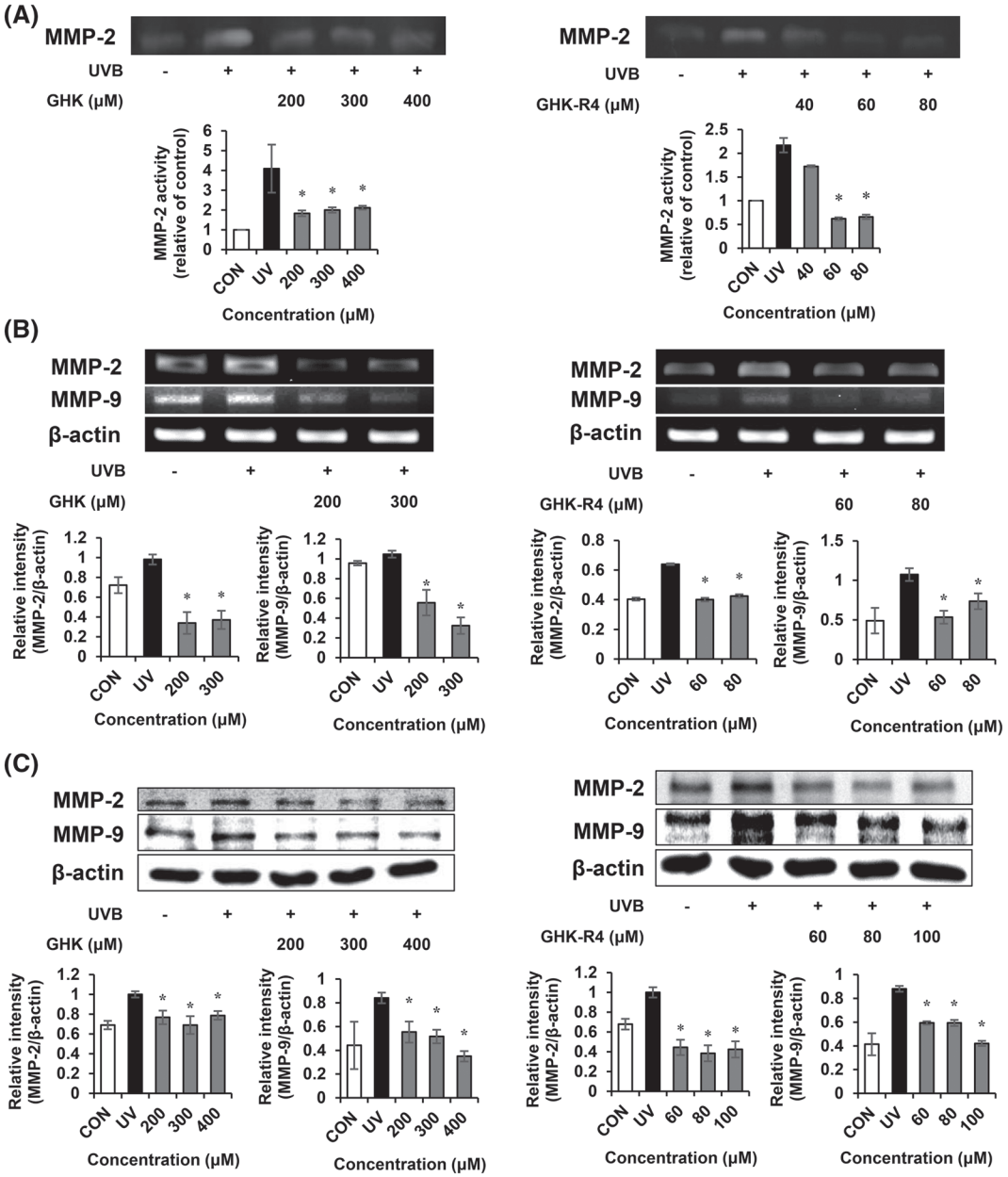

FIGURE 3 (A) Effect of GHK and GHK-R4 on the MMP-2 activity measured by gelatin zymography, (B) on the mRNA level of MMP-2 and MMP-9 by RT-PCR, and (C) the protein expression level of MMP-2 and MMP-9 by western blot. Results are expressed as mean ± SD of independent three tests. $^{*}P < .05$ compared with UVB-irradiated control

hours in blocking solution at RT. After blocking, the membrane was incubated for 18 hours at 4°C with individual primary antibodies diluted in blocking solution. Secondary antibodies conjugated with horseradish peroxidase were then incubated for 50 minutes at RT. The antibodies were visualized using the ECL Plus Western Blotting Detection System. Images were acquired, and band intensities were quantitated using ImageJ.

2.10 | RT-PCR

UVB-damaged Hs68 cells were incubated for 48 hours with individual peptides as described above. Total RNA was isolated from cultures of Hs68 cells using an RNA isolation kit (Nucleo Spin RNA Plus, MN, Düren, Germany). Complementary DNA (cDNA) was synthesized from 0.3 μg of total RNA using a cDNA synthesis kit (Bio-Rad, California) in a thermal cycler (25°C for 5 min, 46°C for 20 min, and 95°C for 1 min; 1 cycle). PCR amplification (95°C for 5 min, 95°C for 30 s, 55°C-60°C for 30 s, 72°C for 1 min, and 72°C 5 min; 23-35 cycles) was then performed. The PCR products were separated by agarose gel electrophoresis using 2% agarose (Applied Biological Materials Inc, Richmond, California) and stained (DNA Staining Bandi-load 6X, SJ Bio Science, Daejeon, Korea). Primers used in this study were MMP-2 sense 5′-CGACCACAGCCAACTACGAT-3′, MMP-2 antisense 5′-GTCA-GGAGAGAGGCCCCATAGA-3′, MMP-9 sense 5′-ATGCCTGCAA CGTGACATC-3′, MMP-9 antisense 5′-ATCGCCAGTACTTCCCATCC-3′, β-actin sense 5′-AGACCTGTACGCCAACACAG-3′, β-actin antisense 5′-CACATCTGCTGGAAGGTGGA-3′.

3 | RESULTS

3.1 | Synthesis of GHK and GHK-R4

All peptides were synthesized using standard Fmoc chemistry-based solid peptide synthesis with 2-chlorotrityl resin. The scheme for synthesis of GHK (GHK-acetate form) and GHK-R4 was depicted in Figure 1.

3.2 | The effects of GHK and GHK-R4 on the viability and proliferation of dermal fibroblasts

Hs68 human dermal fibroblasts were treated with various concentrations of GHK and GHK-R4 for 24 hours and then analyzed by MTT assay. The results showed that the IC_{30} value for GHK was approximately 31.7 mM, while that for GHK-R4 was approximately 5.3 mM. The result showed that the cytotoxicity of GHK-R4 was higher than GHK (Figure 2A).

The proliferative effects were measured by adding 100 μM to 500 μM of GHK and 20 μM to 100 μM of GHK-R4 (Figure 2B).

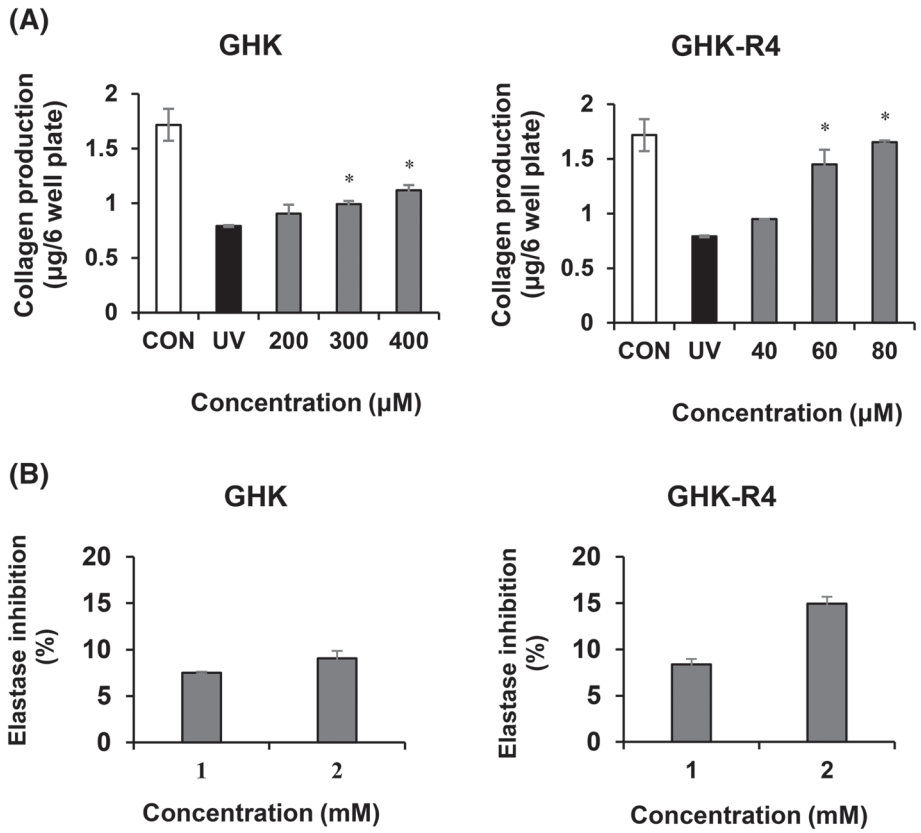

FIGURE 4 (A) Effect of GHK and GHK-R4 on the collagen production by Sircol assay. Values are presented as the mean ± SD of triplicate wells. $^{*}P < .05$ compared with UVB-irradiated control. (B) Inhibitory activity of GHK and GHK-R4 on in vitro elastase activity. Values are presented as the mean ± SD of triplicate wells

The results revealed the in vitro proliferative effect of the peptides to some extent, and that GHK-R4 had higher potency than GHK.

3.3 | Inhibitory effect of GHK and GHK-R4 on UVB-induced MMP expression

The suitable concentration of GHK used for testing MMP expression was assessed to be five to six times higher than that of GHK-R4, on the basis of the relative IC_{30} values shown in Figure 2A. Figure 3A shows that UVB irradiation induced an increase in MMP-2 enzyme activity; however, the MMP-2 activity was inhibited by approximately 55% and 72% upon adding 200 μM GHK and 60 μM GHK-R4, respectively.

The effect of GHK and GHK-R4 on the mRNA expressions of MMP-2 and MMP-9 was also examined by RT-PCR (Figure 3B). The UVB-induced mRNA expressions of MMP-2 and MMP-9 were enhanced; however, their expressions were decreased by GHK and GHK-R4 application.

Next, the protein expressions of MMP-2 and MMP-9 were measured by western blotting in UVB-induced fibroblast cells (Figure 3 C). UVB-induced MMP-2 and MMP-9 protein expression were significantly reduced by application of GHK and GHK-R4. Taken together, the results also suggest that much lower concentrations of GHK-R4 are needed for abrogation of UVB-induced MMP inhibition than GHK at the protein and mRNA level.

3.4 | Effect of GHK and GHK-R4 on the in vitro collagen production and elastase activity

Figure 4A shows that the production of soluble type I procollagen was significantly enhanced by GHK and GHK-R4 in vitro, in comparison with UVB-reduced collagen level in dermal fibroblasts. The type I procollagen increased by approximately 80% at 60 μM GHK-R4, while it increased by 25% at 400 μM GHK over the control UVB-irradiated group. The in vitro inhibition of elastase activity exhibited by GHK and GHK-R4 is shown in Figure 4B. The in vitro elastase assay system consists of porcine pancreatic elastase and *N*-succinyl-(Ala-Ala-Ala)-*p*-nitroanilide as a substrate. Approximately 15% inhibitory activity of 2 mM GHK-R4 for elastase, while 8.5% of 2 mM GHK, suggesting much efficient elastase inhibitory effect of GHK-R4 than GHK.

3.5 | Cellular uptake and in vivo skin penetration of GHK and GHK-R4

The cellular uptake of GHK (GHK-acetate) and GHK-R4 in Hs68 fibroblast was measured without cell fixation in order to prevent

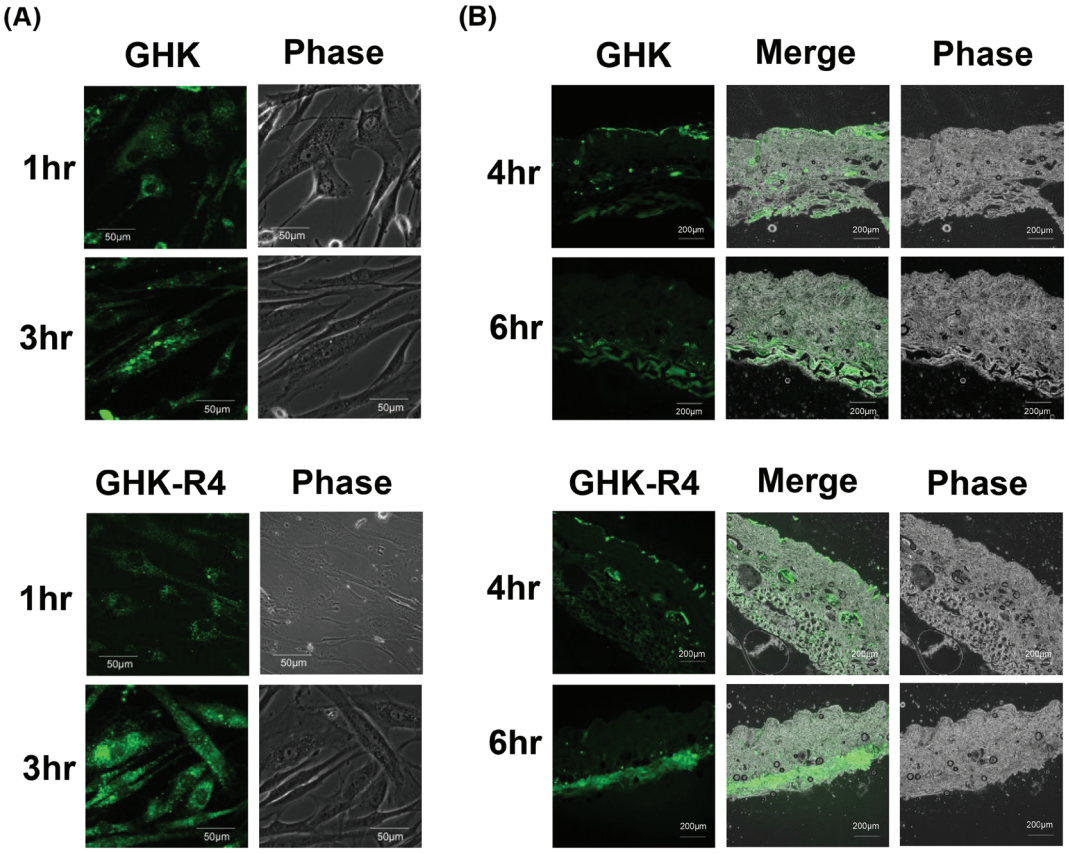

FIGURE 5 (A) The comparison of cellular uptake of GHK and GHK-R4 in Hs68 fibroblasts. The cells were treated with fluorescent 50 μM GHK and GHK-R4 for 1 and 3 h (scale bar = 50 μm). (B) Confocal microscopic images of in vivo skin penetration of GHK and GHK-R4. Hairless mouse skin was treated with GHK and GHK-R4 containing FAM for 4 and 6 h (scale bar = 200 μm)

artifactual redistribution of the cationic peptide following fixation.[13] As shown in Figure 5A, GHK was obviously accumulated in the cytosol at 1 and 3 hours incubation. GHK-R4 was also found in the cytosol at 1 hour; however, GHK-R4 began to enter the nucleus at 3 hours incubation. Thus, some GHK-R4 was found in the nucleus, while the other was found in the cytosol at 3 hours incubation. These results suggest that Arg_4 conjugation accelerates deep penetration of the peptide into cells.

Next, the efficacy of Arg_4 conjugation in enhancing transport of GHK into skin was tested in SKH-1 hairless mice (Figure 5B). At 4 hours following application, the fluorescence derived from GHK was primarily near the outer surface. By contrast, the fluorescence from GHK-R4 penetrated deeper into the skin.

3.6 | Potential dual function of Arg_4

Considering the above results, GHK-R4 exhibited faster penetration into skin and superior in vitro collagen production and MMP inhibition at much lower doses than with GHK. To better understand the underlying reason for the enhanced in vitro antiwrinkle activity of GHK-R4, the activity of Arg_4 alone was measured on the MMP-2 in Hs68 cells as shown in Figure 6. Arg_4 was not cytotoxic at concentrations of approximately 20 mM (Figure 6A). Interestingly, 60 μM and 80 μM Arg_4 alone reduced UVB-induced MMP-2 activity on the gelatin zymographic gel (Figure 6B). Moreover, UVB-induced MMP-2 and MMP-9 expression at the mRNA (Figure 6C) and protein level (Figure 6D) were also reduced by Arg_4 alone. Taken together, the result suggests that Arg_4 might enhance MMP inhibition and dermal delivery at the same time.

4 | DISCUSSION

Dermal delivery of peptides is highly challenging, because they have disadvantageous properties such as high molecular weight and hydrophilicity, and can be rapidly degraded by enzymes.[14] Moreover, a major limitation in transdermal delivery of peptide is to overcome the barrier of the stratum corneum of the epidermis to penetrate the skin.[15] Cell penetrating peptides (CPPs) are short peptides that

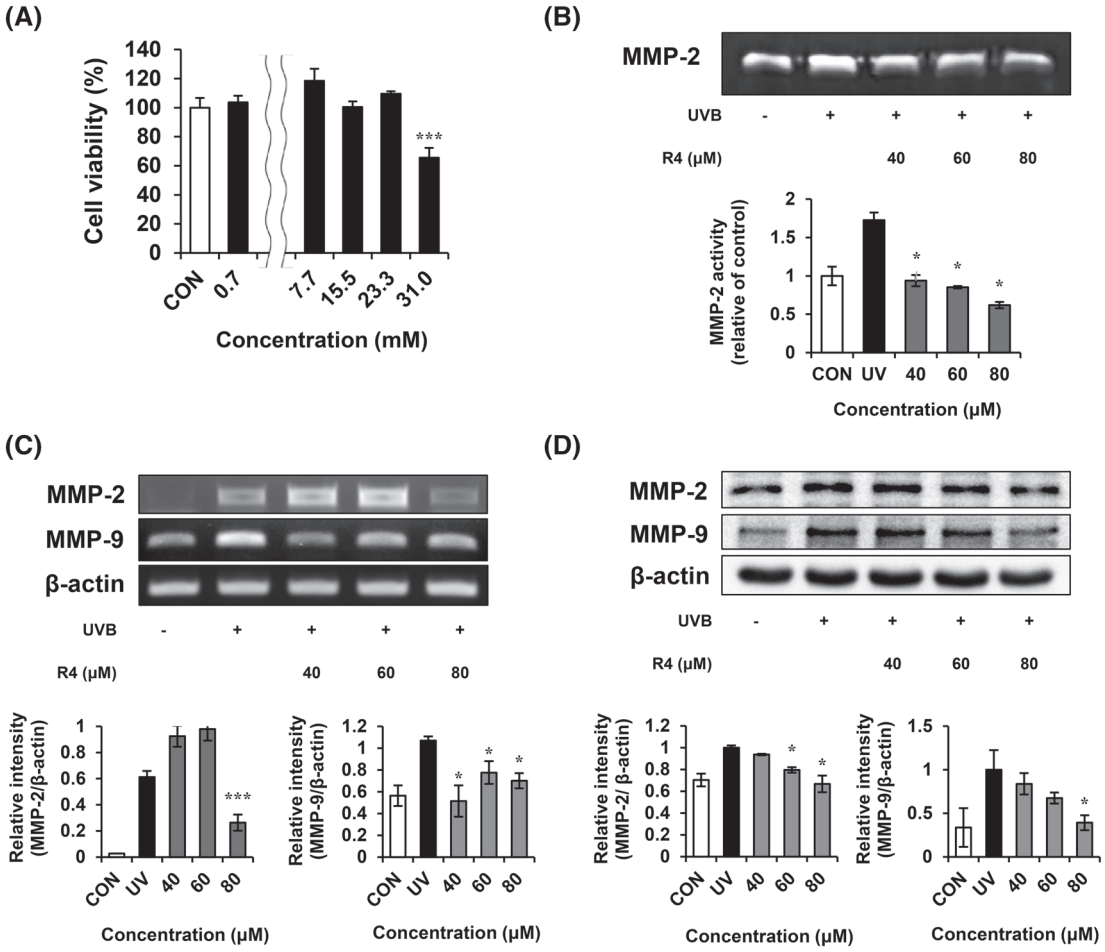

FIGURE 6 (A) The effect of Arg_4 treatment on the cell viability of Hs68 fibroblasts. $^{***}P < .001$. (B) The effect of Arg_4 treatment on the MMP-2 activity analyzed by zymography. $^{*}P < .05$ compared with UVB-irradiation control. The effect of Arg_4 on the mRNA expression of MMP-2 and MMP-9 (C), and the protein expression (D) in UVB-induced Hs68 cells. Results are expression as mean ± SD of independent three tests. $^{*}P < .05$, $^{***}P < .001$ compared with UVB-irradiation control

facilitate cellular uptake of multiple molecules including DNA, chemical compounds, and proteins. There are three classes of CPPs according to their physicochemical properties: cationic, amphipathic, and hydrophobic CPPs.[16] The cationic CPPs, which are composed of arginine, lysine, and histidine, can easily reach the cell membrane because of their cationic characteristics. Arg_7 showed the highest level of cell uptake for gene delivery,[17] while Arg_{11} showed the highest uptake efficiency for prostate cells relative to several other CPPs, including TAT and oligolysine.[18] The others found that Arg_6 to Arg_9 translocated optimally through the cell membrane. Thus, different size and charge of polyarginine might be well suited in delivery diverse materials to different target cells, depending on the association between cell penetration ability and transfection efficiency.[19-21]

In this investigation, low concentrations of GHK (40 μM-80 μM) did not affect MMP activity and MMP expression (data not shown), whereas high concentrations of GHK (200 μM-400 μM) reduced the MMP (Figure 3). Moreover, GHK-R4 and R4 showed higher in vitro antiwrinkle activity at much lower doses than R4-free GHK, as shown in Figures 3 and 6. In addition, Arg_4-conjugated GHK provided efficient penetration in vitro and in vivo, at the same time it showed enhanced in vitro antiwrinkle activity in terms of MMP and elastase inhibition and collagen synthesis, relative to unconjugated GHK. Previous systematic structural investigations on the required number of arginine residues for cellular uptake suggested that less than six arginine residues did not exhibit significant cellular uptake.[22] However, this study showed that GHK-R4 conjugate, with six positive amino acids including histidine (H) and lysine (K), had clear cell penetrating activity, contrary to previous research that reported 4 arginine residues to be insufficient for cell penetration. Moreover, interestingly, 4 Arg itself provided in vitro MMP inhibitory activity. Therefore, 4 Arg seems to have potential dual roles for enhancing GHK function in both cell penetration and antiwrinkle. The superior inhibitory effect with low dose, observed with GHK-R4, might be derived from MMP inhibitory effects of both GHK and Arg_4. In other words, 4 Arg itself might contribute some MMP-2 inhibitory activity of GHK-R4, leading to the synergy we observed. However, currently, it is not elucidated whether GHK is released from the GHK-R4 conjugate in the same fashion as the prodrug system followed by the MMP inhibitory activity, or not. Overall, 4 Arg conjugation might be effective in not only accelerating dermal delivery as a carrier for hydrophilic peptides but also enhancing in vitro antiwrinkle activity of GHK via its own MMP inhibitory activity. We suggest for the first time that 4 Arg conjugated GHK (GHK-R4) might be a more effective cosmeceutical peptide than GHK, which can protect the skin from UVB exposure. A further detailed molecular and cellular study is currently underway into the potential role of 4 Arg residues in cargo delivery and the biological mechanism of 4 Arg and its conjugate. The systematic clinical study is also being conducted.

ACKNOWLEDGEMENTS

This research was supported by Human Resources Exchange Program in Scientific Technology through the National Research Foundation of Korea (NRF) funded by the Ministry of Science and ICT (2018H1D2A2010318). This study was also supported by Soonchunhyang University.

ORCID

Ga-Hee Hur https://orcid.org/0000-0002-2853-8529
A-Reum Ryu https://orcid.org/0000-0002-0330-8620
Mi-Young Lee https://orcid.org/0000-0003-3511-9522

REFERENCES

1. Pickart L, Vasquez-Soltero JM, Margolina A. GHK peptide as a natural modulator of multiple cellular pathways in skin regeneration. *Biomed Res Int*. 2015;2015:648108. 7 pages.
2. Pickart L, Margolina A. GHK-copper peptide in skin remodeling and anti-aging. *SÖFW-J*. 2010;136(6):10.
3. Li H, Low YSJ, Chong HP, et al. Microneedle-mediated delivery of copper peptide through skin. *Pharm Res*. 2015;32(8):2678-2689.
4. Driscoll MS, Kwon EM, Skupsky H, Kwon SY, Grant-Kels JM. Nutrition and the deleterious side effects of nutritional supplements. *Clin Dermatol*. 2010;28(4):371-379.
5. Park JR, Lee H, Kim SI, Yang SR. The tri-peptide GHK-Cu complex ameliorates lipopolysaccharide-induced acute lung injury in mice. *Oncotarget*. 2016;7(36):58405-58417.
6. Godet D, Marie PJ. Effects of the tripeptide glycyl-L-histidyl-L-lysine copper complex on osteoblastic cell spreading, attachment and phenotype. *Cell Mol Biol*. 1995;41(8):1081-1091.
7. McCormack MC, Nowak KC, Koch RJ. The effect of copper tripeptide and tretinoin on growth factor production in a serum-free fibroblast model. *Arch Facial Plast Surg*. 2001;3(1):28-32.
8. Mazurowska L, Mojski M. Biological activities of selected peptides: skin penetration ability of copper complexes with peptides. *J Cosmet Sci*. 2008;59(1):59-69.
9. Förster M, Bolzinger MA, Fessi H, Briançon S. Topical delivery of cosmetics and drugs. Molecular aspects of percutaneous absorption and delivery. *Eur J Dermatol*. 2009;19(4):309-323.
10. Fang YP, Huang YB, Wu PC, Tsai YH. Topical delivery of 5-aminolevulinic acid-encapsulated ethosomes in a hyperproliferative skin animal model using the CLSM technique to evaluate the penetration behavior. *Eur J Pharm Biopham*. 2009;73(3):391-398.
11. Mitchell DJ, Kim DT, Steinman L, Fathman CG, Rothbard JB. Polyarginine enters cells more efficiently than other polycationic homopolymers. *J Pept Res*. 2000;56(5):318-325.
12. Li H, Toh PZ, Tan JY, et al. Selected biomarkers revealed potential skin toxicity caused by certain copper compounds. *Sci Rep*. 2016;6:37664.
13. Richard JP, Melikov K, Vives E, et al. Cell-penetrating peptides. A reevaluation of the mechanism of cellular uptake. *J Biol Chem*. 2003;278(1):585-590.
14. Sommer E, Neubert RHH, Mentel M, Tuchscherer B, Mrestani Y, Wohlrab J. Dermal peptide delivery using enhancer molecules and colloidal carrier systems. Part III: tetrapeptide GEKG. *Eur J Pharm Sci*. 2018;124:137-144.
15. Kwon SS, Kim SY, Kong BJ, et al. Cell penetrating peptide conjugated liposomes as transdermal delivery system of *Polygonum aviculare* L. extract. *Int J Pharm*. 2015;483(1-2):26-37.
16. Borrelli A, Tornesello AL, Tornesello ML, Buonaguro FM. Cell penetrating peptides as molecular carriers for anti-cancer agents. *Molecules*. 2018;23(2):295.

17. Alhakamy NA, Berkland CJ. Polyarginine molecular weight determines transfection efficiency of calcium condensed complexes. *Mol Pharm*. 2013;10(5):1940-1948.
18. Zhou J, Liu W, Pong RC, Hao G, Sun X, Hsieh JT. Analysis of oligoarginine cell-permeable peptides uptake by prostate cells. *Amino Acids*. 2012;42(4):1253-1260.
19. Tokudome Y, Komi T, Omata A, Sekita M. A new strategy for the passive skin delivery of nanoparticulate, high molecular weight hyaluronic acid prepared by a polyion complex method. *Sci Rep*. 2018;8(1):2336.
20. Lopes LB, Ferreira DA, de Paula D, et al. Reverse hexagonal phase nanodispersion of monoolein and oleic acid for topical delivery of peptides: in vitro and in vivo skin penetration of cyclosporin A. *Pharm Res*. 2006;23(6):1332-1342.
21. Suh JS, Lee JY, Chou YJ, et al. Intracellular delivery of cell-penetrating peptide-transcriptional factor fusion protein and its role in selective osteogenesis. *Int J Nanomedicine*. 2014;9:1153-1166.
22. Oh D, NasrolahiShirazi A, Northup K, et al. Enhanced cellular uptake of short polyarginine peptides through fatty acylation and cyclization. *Mol Pharm*. 2014;11(8):2845-2854.

SUPPORTING INFORMATION

Additional supporting information may be found online in the Supporting Information section at the end of the article.

How to cite this article: Hur G-H, Han S-C, Ryu A-R, Eom Y, Kim J-W, Lee M-Y. Effect of oligoarginine conjugation on the antiwrinkle activity and transdermal delivery of GHK peptide. *J Pep Sci*. 2019;e3234. https://doi.org/10.1002/psc.3234